JOURNAL OF APPLIED PHYSICS **109**, 07D730 (2011)

Role of anisotropy configuration in exchange-biased systems

E. Jiménez,[1,a)] J. Camarero,[1,2] P. Perna,[2] N. Mikuszeit,[1] F. J. Terán,[2] J. Sort,[3] J. Nogués,[4] J. M. García-Martín,[5] A. Hoffmann,[6] B. Dieny,[7] and R. Miranda[1,2]
[1]*Departamento de Física de la Materia Condensada and Instituto "Nicolás Cabrera," Universidad Autónoma de Madrid, 28049 Madrid, Spain*
[2]*Instituto Madrileño de Estudios Avanzados en Nanociencia IMDEA-Nanociencia, Campus Universidad Autónoma de Madrid, 28049 Madrid, Spain*
[3]*Institució Catalana de Recerca i Estudis Avançats (ICREA) and Departament de Física, Universitat Autònoma de Barcelona, 08193 Bellaterra, Spain*
[4]*Institució Catalana de Recerca i Estudis Avançats (ICREA) and Centre d'Investigació en Nanociència i Nanotecnologia (ICN-CSIC), Campus Universitat Autònoma de Barcelona, 08193 Bellaterra, Spain*
[5]*Instituto de Microelectrónica de Madrid IMM/CNM-CSIC, 28760 Tres Cantos, Spain*
[6]*Materials Science Division, Argonne National Laboratory, Argonne, Illinois 60439, USA*
[7]*SPINTEC, CEA/CNRS/UJF/INPG, INAC-CEA, F-38054 Grenoble, France*

(Presented 18 November 2010; received 1 October 2010; accepted 2 December 2010; published online 5 April 2011)

We present a systematic study of the anisotropy configuration effects on the magnetic properties of exchange-biased ferromagnetic/antiferromagnetic (FM/AFM) Co/IrMn bilayers. The interfacial unidirectional anisotropy is set extrinsically via a field cooling procedure with the magnetic field misaligned by an angle β_{FC} with respect to the intrinsic FM uniaxial anisotropy. High resolution angular dependence in-plane resolved Kerr magnetometry measurements have been performed for three different anisotropy arrangements, including collinear $\beta_{FC} = 0°$ and two opposite noncollinear cases. The symmetry breaking of the induced noncollinear configurations results in a peculiar nonsymmetric magnetic behavior of the angular dependence of magnetization reversal, coercivity, and exchange bias. The experimental results are well reproduced without any fitting parameter by using a simple model including the induced anisotropy configuration. Our finding highlights the importance of the relative angle between anisotropies in order to properly account for the magnetic properties of exchange-biased FM/AFM systems. © *2011 American Institute of Physics*. [doi:10.1063/1.3562507]

Prospects for control and design of desirable magnetic behavior for ferromagnetic (FM)/antiferromagnetic (AFM) systems depend upon a clear understanding of the key parameters governing the exchange coupling at the interface, referred to as exchange bias.[1] The most striking feature of these systems is the shift of the FM hysteresis loop along the magnetic field axis,[2] which is widely used to pin the magnetization direction of a FM reference layer in spintronic devices. Among others, coercivity enhancement and asymmetric magnetization reversal are usually observed features,[3] and often manifest themselves very differently for various material combinations. In addition, these effects also depend on the magnetic field orientation, hence exhibiting a complex phase diagram.[4–10] It is well established that the spin arrangement at the FM/AFM interface plays an essential role in understanding these effects but, despite extensive research, there are still ongoing controversies about the fundamental mechanisms governing them. For instance, ad-hoc phenomenological anisotropies are often postulated without microscopic justification or sufficient experimental evidence to address the magnetic properties in exchange-biased systems.

Recently, we have shown that the angular dependence of the magnetic properties contains an unique fingerprint of the various effective anisotropies of exchange-biased systems.[4,11,12] In particular, the angular dependence of the exchange bias ($\mu_0 H_E$), coercivity ($\mu_0 H_C$), and magnetization reversal, including its asymmetric behavior, depends on the ratio of the involved anisotropies[4] as well as on their relative orientation.[11,12] The latter can be promoted either intrinsically by interfacial frustration[10,11] or extrinsically via patterning[5,6] and/or special field cooling (FC) procedures.[12–16] Here we compare the angular dependence of the magnetic properties of a 18 nm Co/5 nm IrMn bilayer with three tailored anisotropy configurations, including collinear and two opposite noncollinear configurations.

The reference Co layer and the Co/IrMn bilayer were deposited via sputtering at room temperature on thermally oxidized Si substrates. A buffer layer of 5 nm Ta deposited at oblique incidence was employed to favor [111] texture as well as to promote a well-defined uniaxial anisotropy, K_U, in the FM layer. With this method the easy axis of magnetization of the FM layer is in the direction perpendicular to the plane of incidence of the sputtered Ta buffer layer.[11] Finally, the samples were capped by 2 nm of Ta to prevent oxidation. The induced interfacial unidirectional anisotropy, K_E, was set after warming the bilayer to 420 K and FC to room temperature (RT) in a 0.3 T external field misaligned by an angle β_{FC} with respect to K_U. Three different anisotropy configuration were set by using $\beta_{FC} = 0°$ (collinear) and $\beta_{FC} = -20°$ and $+18°$ (noncollinear). Angular dependent, high

a)Electronic mail: erika.jimenez@uam.es.

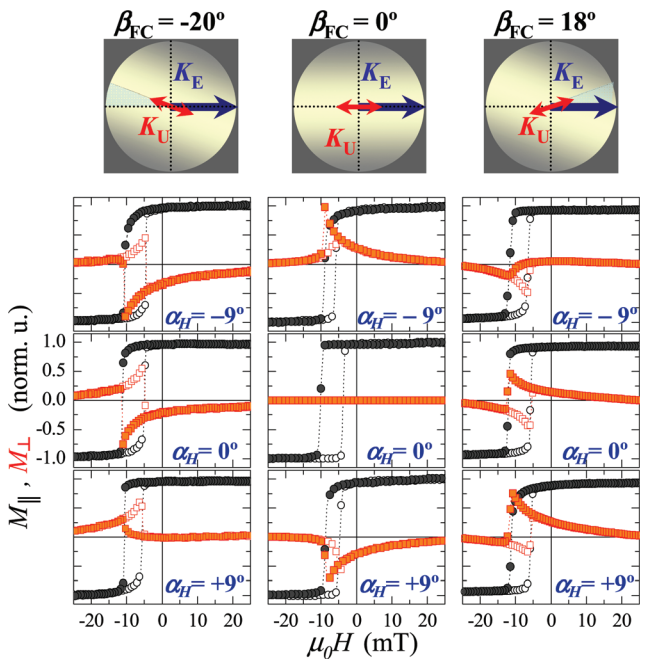

FIG. 1. (Color online) Parallel and transversal hysteresis loops at selected applied field angles, α_H, for exchange-biased 18 nm Co/5 nm IrMn bilayers with different anisotropy configuration, schematically shown on top, including collinear ($\beta_{FC} = 0°$, central column graphs) and noncollinear (left, $\beta_{FC} = -20°$ and right, $\beta_{FC} = +18°$) cases. The experimental $M_{||}$ (H) and $M_\perp$ (H) loops were acquired simultaneously and are represented by circles and squares, respectively. The two branches of the hysteresis are depicted with closed and open symbols for decreasing and increasing fields, respectively.

resolution, in-plane resolved Kerr magnetometry measurements were performed at RT to study the dependence of the reversal of both in-plane magnetization components, i.e., parallel ($M_{||}$) and transverse ($M_\perp$) magnetization components with respect to the applied field angle α_H, where $\alpha_H = 0°$ is defined as the FC direction.

The characteristic anisotropy axis and the reversal processes can be determined directly by a simple inspection of the parallel and transversal loops, highlighting the importance of vectorial magnetometry. For instance, Fig. 1 shows representative in-plane resolved magnetization loops for a 18 nm Co/5 nm IrMn bilayer with collinear (central column graphs) and the two opposite noncollinear (left and right column graphs) anisotropy configurations acquired at selected α_H angles around the FC direction. In general, sharp (irreversible) transitions and/or smoother (fully reversible) transitions are observed in both $M_{||}(H)$ and $M_\perp(H)$ loops. The relative weight of these two contributions depends on α_H. As expected for extended magnetic systems, the sharp transitions correspond to nucleation and further propagation of magnetic domains, whereas the reversible transitions correspond to rotation processes. This has been recently confirmed by Kerr microscopy measurements.[17]

In particular, for $\alpha_H = 0°$, the central graphs of Fig. 1 show similar $\mu_0 H_E$ and $\mu_0 H_C$ values for the three anisotropy configurations as well as that the magnetization behaves symmetrically whether the field is swept along (increasing field branch) or against (decreasing field branch) the FC direction. However, the reversal in each system takes place in a different fashion. $M_{||}$ reverses mainly via a sharp irreversible transition for all cases, indicating that the reversal is mainly governed by nucleation and propagation of magnetic domains. In contrast, while $M_\perp = 0$ in the whole field loop for the collinear configuration, clear hysteresis with both smooth reversible and sharp irreversible transitions are observed for the two noncollinear cases. This indicates that during the sharp transitions the magnetization of the nucleated magnetic domains is aligned parallel to the external field for the collinear configuration while it is nonparallel for the noncollinear cases. In addition, the different sign of the $M_\perp(H)$ loop of the opposite noncollinear cases indicates that the FM anisotropy direction dictated the reversal rotation pathway of $M_\perp$, i.e., the magnetization rotates in plane in a clockwise and counterclockwise sense for $\beta_{FC} = -20°$ and $\beta_{FC} = +18°$, respectively.

For $\alpha_H \neq 0°$, in general, the magnetization follows a different pathway for each branch of the hysteresis loop, i.e., asymmetric reversal. However, several remarkable differences are identified for the three anisotropy configurations, as shown in the top and bottom graphs of Fig. 1. The asymmetric reversal behavior shows up as by differently rounded $M_{||}$ transitions and different maximum values of $M_\perp$ observed in the decreasing and increasing field branches of the hysteresis loops. Interestingly, the asymmetry and the differences between the anisotropy configurations becomes more obvious in the $M_\perp(H)$ loop. For instance, while the maximum of $M_\perp$ is significantly larger during the descending branch for the collinear case, this can be found in either descending or ascending branches of the hysteresis loop for the noncollinear cases, depending on the sign of α_H. Moreover, $M_\perp$ reverses just in one semicircle [i.e., $M_\perp(H)$ can be either only positive or negative, for all H] for the collinear case, whereas for the noncollinear cases it can reverse in one or in both semicircles. In addition, the reversal asymmetry is not symmetric around the FC direction in the noncollinear case. While for the collinear case the maximum $M_\perp$ signal is always found in the descending branch of the hysteresis loop, for the noncollinear cases this can be found in either descending or ascending branches, depending on the sign of the applied magnetic field angle with respect to the FC direction. This indicates that rotation processes are always more relevant when the field is swept against the FC direction in the collinear case, whereas it depends on both α_H and β_{FC} for the noncollinear case. Finally, it has to be noticed that the magnetization reversal for the two opposite noncollinear configurations behaves similarly if magnetization loops acquired at different sign of α_H are compared, i.e., $M_\perp(H, +\alpha_H, +\beta_{FC}) \approx -M_\perp(H, -\alpha_H, -\beta_{FC})$.

The symmetry breaking of the noncollinear configuration can clearly be observed in the angular evolution of $\mu_0 H_E$ and coercivity $\mu_0 H_C$ shown in Fig. 2. For instance, in clear contrast with the collinear case (central graph), both coercivity and exchange bias are not symmetric around $\alpha_H = 0°$ for the noncollinear cases (top and bottom graphs), i.e., $H_C(-\alpha_H) \neq H_C(+\alpha_H)$ and $H_E(-\alpha_H) \neq H_E(+\alpha_H)$. The coercivity displays a plateau around the FC direction angle, which coincides with the occurrence of $M_\perp$ reversal in both semicircles. In a similar way compared to the collinear case,

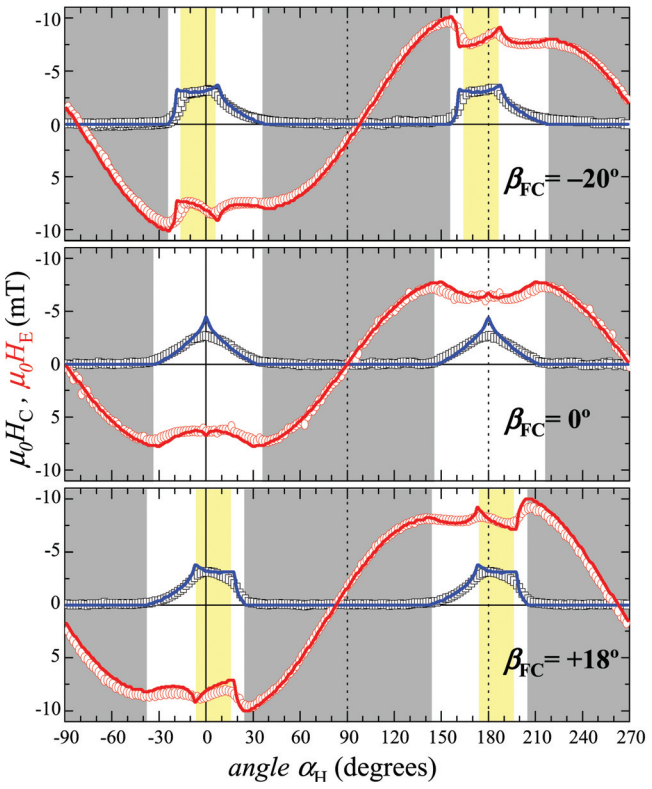

FIG. 2. (Color online) Angular dependence of exchange bias, H_E, and coercivity, H_C, of 18 nm Co/5 IrMn bilayers with different anysotropy configurations, including collinear ($\beta_{FC} = 0°$, central graphs) and noncollinear (top $\beta_{FC} = -20°$ and bottom $\beta_{FC} = +18°$) cases. The symbols are the experimental values derived from Kerr measurements as those shown in Fig. 1. Continuous lines are the simulated curves obtained with the SW model with no adjustable parameters, by using the tailored anisotropy configurations. The range of angles where only reversible processes take place during the reversal are marked by dark gray shadowed areas. The angular range around the FC direction where $M_\perp$ reverses in both semicircles is also highlighted by a light shadowed area.

the angular range where an asymmetric reversal behavior is observed coincides with the onset of coercivity, i.e., $H_C \neq 0$, the onset of reversible processes, and the maximum of exchange bias. However, this angular range is also not symmetric around the FC direction. Finally, similar to the magnetization reversal behavior, the features of the two opposite noncollinear configurations are mirrored around the FC direction, i.e., $H_C(+\alpha_H, +\beta_{FC}) \approx H_C(-\alpha_H, -\beta_{FC})$ and $H_E(+\alpha_H, +\beta_{FC}) \approx H_E(-\alpha_H, -\beta_{FC})$.

All the experimentally observed magnetic behaviors have been reproduced within the coherent rotation Stoner–Wohlfarth (SW) model without any fitting parameter,[4] by using the experimental K_U, K_E, and β_{FC}. The values given by the model agree well with the experimental data, as shown by the solid lines in Fig. 2, except for the overestimated coercivity around $\alpha_H = 0°$ and $\alpha_H = 180°$, i.e., easy axis direction. In these regions, as discussed earlier, irreversible behavior involving nucleation and further propagation of magnetic domains become more important leading to the discrepancy with the calculation.

In summary, a number of asymmetries related to collinear and noncollinear anisotropy configuration have been identified and characterized in the reversal modes as well as in both coercivity and exchange bias. The anisotropy configuration was set in a control way via a FC procedure with the magnetic field misaligned with respect to intrinsic FM anisotropy. Our findings highlight the importance of the relative angle between anisotropies in exchange-biased FM/AFM and open new paths for the tailoring of exchange-biased systems.

This work was supported in part by the Spanish MICINN through Project Nos. CSD2007-00010, MAT2010-21822, and MAT2010-20616-C02 and by Comunidad de Madrid and the Generalitat de Catalunya through Project Nos. S2009/MAT-1726 and 2009-SGR-1292, respectively. Work at Argonne was supported by the U.S. Department of Energy-Basic Energy Sciences under Contract No. DE-AC02-06CH1357.

[1]W. H. Meiklejohn and C. P. Bean, Phys. Rev. **102**, 1413 (1956).
[2]See reviews, J. Nogués and I. K. Schuller, J. Magn. Magn. Mater. **192**, 203 (1999); A. E. Berkowitz and K. Takano, *ibid*. **200**, 552 (1999).
[3]F. Radu and H. Zabel, Springer Tracts Mod. Phys. **227**, 97 (2008).
[4]J. Camarero, J. Sort, A. Hoffmann, J. M. García-Martín, B. Dieny, R. Miranda, and J. Nogués, Phys. Rev. Lett. **95**, 057204 (2005).
[5]A. Hoffmann, M. Grimsditch, J. E. Pearson, J. Nogués, W. A. A. Macedo, and I. K. Schuller, Phys. Rev. B. **67**, 220406 (2003).
[6]S. H. Chung, A. Hoffmann, and M. Grimsditch, Phys. Rev. B. **71**, 214430 (2005).
[7]F. Radu, A. Westphalen, K. Theis-Bröhl, and H. Zabel, J. Phys.: Condens. Matter. **18**, L29 (2006).
[8]M. J. M. Pires, R. B. de Oliveira, Jr, M. D. Martins, J. D. Ardisson, and W. A. A. Macedo, J. Phys. Chem. Solids **68**, 2398 (2007).
[9]A. Tillmanns, S. Oertker, B. Beschoten, G. Güntherodt, J. Eisenmenger, and I. K. Schuller, Phys. Rev. B **78**, 012401 (2008).
[10]J. McCord, C. Hamann, R. Schäfer, L. Schultz, and R. Mattheis, Phys. Rev. B. **78**, 094419 (2008).
[11]E. Jiménez, J. Camarero, J. Sort, J. Nogués, A. Hoffmann, N. Mikuszeit, J. M. García-Martín, B. Dieny, and R. Miranda, Phys. Rev. B **80**, 014415 (2009).
[12]E. Jiménez, J. Camarero, J. Sort, J. Nogués, A. Hoffmann, F. J. Teran, P. Perna, J. M. García-Martín, B. Dieny, and R. Miranda, Appl. Phys. Lett. **95**, 122508 (2009).
[13]J. Nogués, D. Lederman, T. J. Moran, and I. K. Schuller, Phys. Rev. Lett. **76**, 4624 (1996).
[14]J. Nogues, T. J. Moran, D. Lederman, I. K. Schuller, and K. V. Rao, Phys. Rev. B **59**, 6984 (1999).
[15]S. Brück, J. Sort, V. Baltz, S. Suriñach, J. S. Muñoz, B. Dieny, M. D. Baró, and J. Nogués, Adv. Mater. **17**, 2978 (2005).
[16]J. Olamit, Z. P. Li, I. K. Schuller, and K. Liu, Phys. Rev. B **73**, 024413 (2006).
[17]E. Jiménez, C. Rodrigo, A. Hrabec, S. Pizzini, F. J. Teran, J. Vogel, P. Perna, N. Mikuszeit, J. Camarero, and R. Miranda (unpublished).